

Thermally stimulated polarization and depolarization processes in $\text{Al}_2\text{O}_3\text{:Mg}$

R. Vila

Centro de Investigaciones Energéticas, Medioambientales y Tecnológicas, Instituto de Investigación Básica, Avenida Complutense 22, 28040 Madrid, Spain

M. Jiménez de Castro

Consejo Superior de Investigaciones Científicas, Instituto de Ciencia de Materiales, Serrano 113, 28006 Madrid, Spain

(Received 3 August 1993)

Thermally stimulated polarization (TSP) and depolarization current measurements in as-cut as well as in oxidized magnesium-doped aluminum oxide show a huge peak at around 265 K, another one at 245 K, and a broadband at higher temperatures. They are related to the presence of Mg_{Al}^x centers (substitutional magnesium ions with a hole trapped at a neighboring oxygen ion) and originate from the thermally activated ionization of these centers, which release holes. The current-voltage curves and the TSP results related to the main polarization process show that this is due to the formation of blocking contacts at the sample-electrode interfaces.

I. INTRODUCTION

Optical-absorption and electron-spin resonance (ESR) studies in magnesium-doped aluminum oxide have shown that quenching of samples from above 1200 K in an oxidizing atmosphere induces Mg_{Al}^x defects,¹ which consist of a substitutional Mg^{2+} ion with a trapped hole localized on one of the six oxygen ions surrounding the magnesium impurity.² These centers are stable above room temperature. Ionizing irradiation below room temperature also creates the same defects,² but they are thermally unstable above 200 K by hole release from the neutral acceptors Mg_{Al}^x .^{1,3,4} The charge of the Mg_{Al}^x defects is mainly compensated by $V_{\text{O}}^{\cdot\cdot}$ and $\text{Al}_i^{\cdot\cdot\cdot}$ (using the Kröger and Vink notation⁵). The thermal stability of the quenching-induced centers is postulated to be due to the formation of magnesium-rich inclusions from $(\text{MgO})_x\text{:Al}_2\text{O}_3$ spinel precipitates involving oxygen penetration along dislocations or subgrain boundaries followed by its slow penetration into subgrains.¹ This is the "microgalaxy" model proposed by Chen *et al.*⁶ to explain in MgO:Li the formation by oxidizing quenching of Li_{Mg}^x centers, which behave in the same way as the Mg_{Al}^x centers. According to this model the initial leakage of trapped holes will result in a corresponding negative charge (Mg_{Al}^x centers) in the inclusions that prevents further leakage, causing the remaining Mg_{Al}^x centers to be stable well above room temperature. Chemical reactions leading to the formation by quenching of these stable centers have been given by Wang *et al.*¹ The fact that spinel precipitates have been seen to decorate dislocations in $\text{Al}_2\text{O}_3\text{:Mg}$ together with the very high diffusion rates at rather low temperatures indicates that these reactions occur near dislocation lines.

The final situation corresponds to a *p*-type semiconductor embedded in an insulating matrix, since Li_{Mg}^x or Mg_{Al}^x can thermally ionize to produce holes. From the experimental results obtained in MgO:Li by using both the thermally stimulated depolarization technique (developed

by Bucci, Fieschi, and Guidi⁷) and dielectric-relaxation measurements as a function of frequency, it has been proposed that Maxwell-Wagner polarization occurs in these regions.⁸ Therefore, it is interesting to know whether such a mechanism takes place in $\text{Al}_2\text{O}_3\text{:Mg}$. The thermally stimulated polarization (TSP) and depolarization (TSD) techniques have been employed in this work. TSP and TSD signals like those observed in MgO:Li have also been obtained here, but our results indicate that the main process is due to interfacial polarization at the sample electrodes. The Mg_{Al}^x centers are related to this process.

II. EXPERIMENT

Mg -doped Al_2O_3 single crystals grown by the Verneuil method were used in this work. They were kindly supplied by Dr. B. Salce (Centre d'Etudes Nucléaires de Grenoble, France). Impurity chemical analysis shows that the magnesium content varies between 20 and 40 ppm from batch to batch. Other checked impurities were Ti (10 ppm), Cr (<21 ppm), and Fe (<13 ppm). Samples of about $5 \times 5 \times 0.5 \text{ mm}^3$ were cut from the Mg -doped aluminum oxide crystals. Electrodes of either indium foil or evaporated metals (platinum, gold, or aluminum) were employed. All types of electrodes gave the same qualitative results, so indium foil was most used.

Thermal quenches were made by heating samples in air at a given temperature for a preset period of time and dropping them into liquid nitrogen. This procedure produces less cracks than quenching in water. A pulsed thermal annealing method was used to study the thermal stability of quenching-induced effects: after each heating pulse (10 min in air) up to increasing temperature values followed by a slow cooling down to room temperature, the optical-absorption and the TSP (or TSD) spectra were obtained.

TSP and TSD measurements between 20 and 320 K were performed in a Displex CSW-202 closed-cycle refri-

generation system at a heating rate of 0.13 K s^{-1} . A Keithley 617 electrometer was used for electric-current measurements. Either a Fluke 415 B high-voltage power supply for the TSD measurements or the electrometer internal-voltage source for the TSP ones were employed for sample polarization. In TSD measurements, after polarizing near room temperature with an electric field E_p of $500\text{--}40\,000 \text{ V cm}^{-1}$, the sample is allowed to cool down to 20 or 77 K, the electric field is then removed and the depolarization currents are measured during the subsequent linear heating run by connecting the electrometer to the sample electrodes. In TSP measurements the sample is linearly heated with an applied electric field. Optical-absorption spectra were taken at room temperature in a Cary 17 spectrophotometer. An Apple Macintosh IIcx computer with multipurpose input-output and GPIB cards controlled the experimental system and the data acquisition.

III. RESULTS

A. TSP and TSD spectra

The optical-absorption spectrum of the as-cut Mg-doped aluminum oxide samples shows a broadband at 480 nm (2.68 eV) due to Mg_{Al}^x centers.¹ The TSP and TSD spectra of these samples are similar to those of air-quenched samples (see below). On annealing in argon atmosphere up to 1500 K both the 480-nm band and the TSP-TSD peaks disappear. Quenching a previously annealed sample in air from above 1250 K induces again the 480-nm band and the TSP and TSD spectra. A TSP spectrum for a low polarizing electric field (500 V cm^{-1}) and a TSD spectrum of a sample polarized at 280 K are presented in Fig. 1. They show a huge peak at about 265 K, which will be referred to as peak B. Its maximum varies in temperature depending on the experimental conditions (see later). When the sample is polarized at low temperature its TSD spectrum (see also Fig. 1) reveals

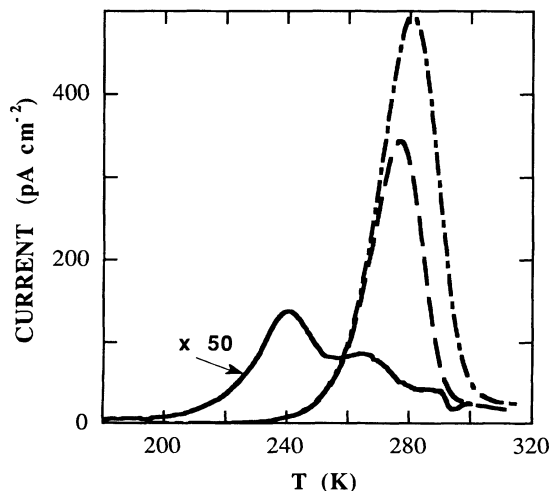


FIG. 1. TSP (---) and TSD (- · -) spectra ($T_p = 280 \text{ K}$) of an $\text{Al}_2\text{O}_3\text{:Mg}$ sample quenched in air from 1270 K ($E_p = 500 \text{ V cm}^{-1}$). TSD spectrum of a sample polarized at 210 K (—).

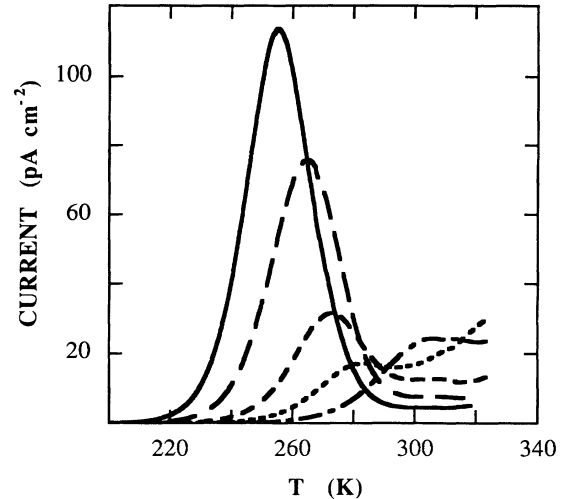


FIG. 2. TSD spectra after polarizing a quenched $\text{Al}_2\text{O}_3\text{:Mg}$ sample for a 5-K interval during cooling, for different temperatures ranging between 290 and 250 K.

another peak at about 245 K (peak A) whose intensity is many times lower than that of peak B. In this case the peak B intensity is strongly reduced because of the very low polarization temperature.

Peak B is broadened on its high-temperature side and its intensity does not reach the zero value below 320 K, which is the upper limit of our experimental setup. This is due to the presence of a wide distribution of low-intensity peaks (hereafter referred to as the HT region), as it can be seen by using the thermal sampling method with a "polarization window" of 5 K: the sample is polarized during cooling at some temperature, the electric field being removed when the sample temperature is 5 K below the initial polarization temperature. The sample is then allowed to cool well below this polarization-temperature range. This procedure allows process B to be depolarized during cooling (after the electric-field removal), permitting us, therefore, to isolate the high-temperature processes in the subsequent heating run. Some spectra obtained in this way, corresponding to different polarization-temperature ranges, are plotted in Fig. 2. They show that the HT region is actually a distribution of TSD peaks. Due to the temperature range of our experimental setup the HT region could not be thoroughly scanned. A complete study of this process was, thus, not possible, as it is also the case of peak A because of its strong overlapping with peak B and of the very small height ratio. This paper is then mostly based on the experimental data obtained for peak B, which is by far the most important process.

TSP measurements were also made with polarizing fields higher than 2000 V cm^{-1} . Some of the obtained results are shown in Fig. 3. The first TSP run shows the peak B over a background current which strongly increases with the temperature. Cooling the sample after this first TSP run and making a new measurement again, both with the electric field on, does not give rise to any peak, but the background current is still observed. The

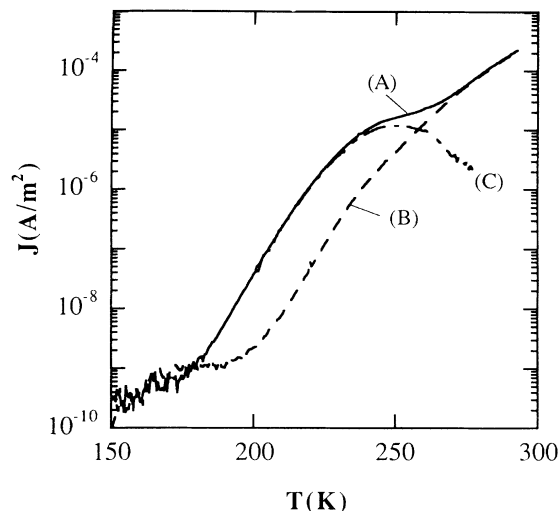


FIG. 3. TSP spectrum of $\text{Al}_2\text{O}_3\text{:Mg}$ for an applied electric field of $11\,300\text{ V cm}^{-1}$ (A). Spectrum obtained after cooling the sample and heating it again both with this field on (B) and the difference between both spectra (C). The sample was previously quenched from 1920 K.

difference between these two spectra gives the main TSP peak and the HT region, as can also be seen in this figure.

B. Activation parameters

A fitting method⁹ has been used to calculate the activation energy E_a and the preexponential factor τ_0 of peak B. This method allows us to fit to a first-order process even peaks whose high-temperature half side is affected by the presence of another peak. It also permits one to obtain the fitted peak isolated from these possible high-temperature contributions and, therefore, the area under

the studied peak can be calculated without any contribution of other processes. All measurements fit well to a first-order-kinetics process for its low-temperature side. The high-temperature side is always slightly wider than that corresponding to a first-order peak. However, fittings for all measurements shown below lead to similar activation-energy values: $E_a = 0.67 \pm 0.04\text{ eV}$. τ_0 does depend on the experimental conditions, its order of magnitude being 10^{-11} s . Peak A cannot be well isolated due to its strong overlapping with peak B. However, fitting both peaks simultaneously in TSD measurements with a polarizing temperature T_p of 215 K gave an activation energy value for peak A of $0.58 \pm 0.04\text{ eV}$. The actual value may be higher because the peak is broadened and then is probably better fitted by a Gaussian distribution of parameters. Moderate broadenings have been seen to increase this energy value by about 0.1 eV. The order of magnitude of τ_0 is 10^{-10} s .

The TSP-TSD activation parameters can also be calculated by performing polarization-current measurements at a constant temperature. The results obtained between 240 and 320 K in a sample quenched from 1270 K are plotted in Fig. 4. All curves (each one corresponding to a measurement temperature) are displaced along both X and Y axes in order that all of them are superimposed in a unique "master" curve.¹⁰ The current versus time curve can be split into two time regions: at low times, the relaxation process follows very well an exponential behavior whereas a t^{-n} law masks the exponential tail at higher times. This indicates that we are dealing with a near Debye-type process at low temperatures. This is an extreme case of the dielectric-relaxation-universal law, whose exponential characteristic function is represented in the logarithmic plot as a continuously curving line whose slope passes through -1 at $t = 1/\omega_p$, ω_p being the resonance frequency at a given temperature.¹⁰ In the

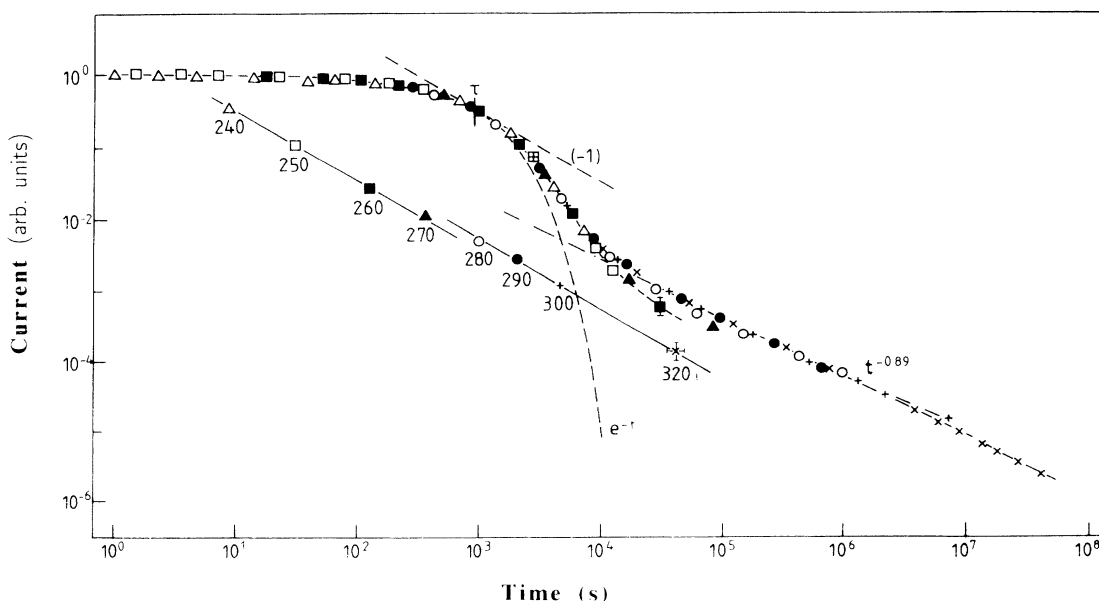


FIG. 4. Isothermal polarization curves at several temperatures. The results for each temperature have been normalized by shifting laterally each curve into coincidence. The full line represents the fit of the locus of the reference point of each curve.

temperature range between 295 and 320 K the polarization curve becomes a unique straight line whose slope is $n=0.89$. This region corresponds to the HT process, where a distribution of peaks seems to occur.

The amounts of the curve displacements in Fig. 4 as a function of $1/T$ can also be fitted to a straight line at low temperatures, from which the activation parameters can be calculated.¹⁰ The obtained values are $E_a=0.67\pm 0.03$ eV and $\tau_0\approx 5\times 10^{-12}$ s, in very good agreement with the TSP-TSD results. It is important to point out that this procedure to calculate the activation energy does not require any assumption on the process-kinetics order. Therefore, there is a close parallelism between the near-first-order TSP peak *B* and the time-domain exponential decay on one hand, and between the broad peak distribution (HT region) and the universal-relaxation-law decay (t^{-n}) on the other. It is a known fact that a superposition of several exponential decays due to a trap distribution leads to a t^{-n} law decay.¹¹

C. General dependences of the TSP parameters

Besides their dependence on the thermal treatments which will be presented below, the area and the position of peak *B* depend on the sample thickness d and on the applied voltage V_p in the following way.

Figure 5 presents the peak *B* area (in electric charge per unit electrode area, that is, the sample polarization P_0) divided by the applied electric field $E_p (=V_p/d)$ plotted against d . A linear dependence of the TSP results on the sample thickness is seen to occur for both as-cut and air-quenched samples.

The area under peak *A* (in TSD measurements with $T_p=215$ K) seems to grow linearly with V_p . This is not the case of peak *B*, whose area is approximately proportional to $V_p^{1/2}$, as it can be seen in Fig. 6. It is important to point out that these consecutive measurements must be made in an increasing voltage order, otherwise, hysteresis effects could appear, as it has been observed here.

The temperature at the maximum, T_m , of peak *B* shows a monotonous increase with d . Although such a behavior could at first glance be ascribed to a tempera-

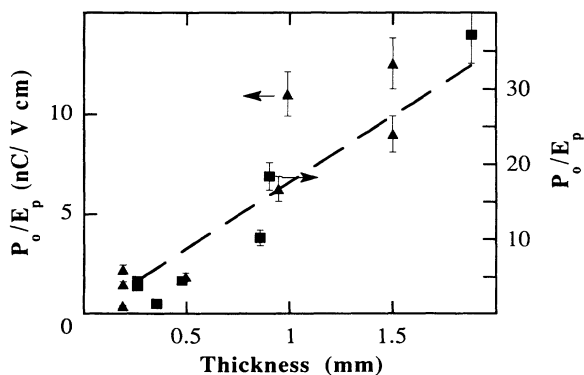


FIG. 5. Values of P_0/E_p (P_0 being the total electric charge per unit electrode area and E_p being the applied electric field) against the sample thickness for as-cut (▲) and quenched (■) samples. ($E_p=500$ V cm⁻¹.)

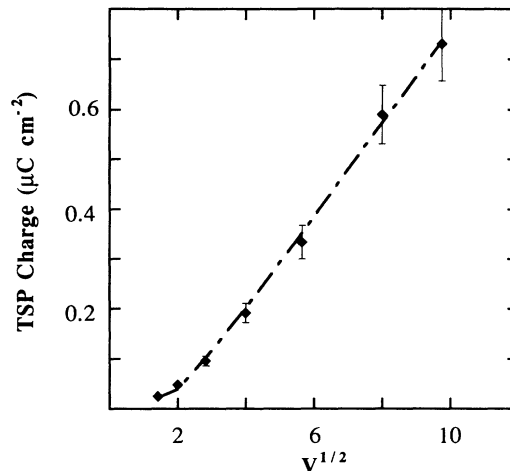


FIG. 6. Dependence of the peak *B* area on the applied voltage. The dotted line represents the fitting to the theoretical curve according to Eq. (3).

ture gradient across the sample, the shift in T_m (around 20 K for thickness ranging between 0.2 and 1.8 mm) is too large to be explained by this effect. Experimental values for this gradient measured in a 1-mm-thick sample gave values lower than 2 K in all the temperature range of the TSP run.

Finally, T_m decreases with increasing V_p . This has been observed to occur in all the studied samples and is more clearly seen in the case of TSD experiments, where high-voltage polarization is used (as a numerical value, a change of three orders of magnitude in the voltage induces a shift of about 10 K in the peak position). As a consequence of this effect the obtained activation energy is a bit lower at high-polarization fields. This voltage effect has a “memory effect” in the sense that the exact value of T_m depends upon voltage values used earlier.

D. Effects of thermal treatments on the TSP spectra

The evolution of peak *B* when varying the experimental conditions in the oxidizing quenches after annealing the samples in argon atmosphere has been studied. A straight line with slope 1.25 is obtained when plotting the growth of the peak *B* area against the heating period at 1270 K before quenching.¹² Saturation is reached for a heating time of about 200 min, this being shorter for higher quenching temperatures: saturation occurs in about 20 min at 1520 K. The overall TSP shape is practically unaffected by increasing the heating period. For peak *B*, T_m , and thus τ_0 , becomes slightly lower as the heating period is larger, the E_a value being always quite the same. The optical absorption at 480 nm also grows with the heating period. To obtain the evolution of TSP with the quenching temperature T_Q using results from different samples, the peak *B* area divided by the applied voltage, i.e., the capacitance, has been taken into account because our results indicate that this quantity does not depend on the sample thickness. Since the amount of polarization varies from one sample to another for the same

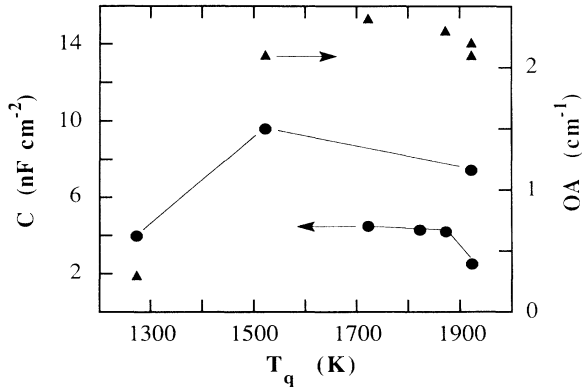


FIG. 7. Dependence on the quenching temperature of the sample capacitance (\bullet) ($V_p = 25$ V, points corresponding to the same sample are joined by a full line) and of the 480-nm optical-absorption-band height (\blacktriangle).

experimental conditions (this could be due to differences in the impurity concentration, dislocation density, etc.), it is difficult to draw a general curve. Figure 7 shows some of the obtained results. It can be said that the capacitance as well as the 480-nm optical absorption grows with T_Q up to about 1600 K. Both seem to reach saturation and then to decrease slightly for very high T_Q values. The optical-absorption saturation value corresponds to a Mg_{Al}^x -center concentration of about $3 \times 10^{17} \text{ cm}^{-3}$ (6 ppm). For samples of the same thickness, the larger the T_Q value the lower the T_m value, this shift in T_m being about 35 K for T_Q ranging between 1300 and 1900 K.

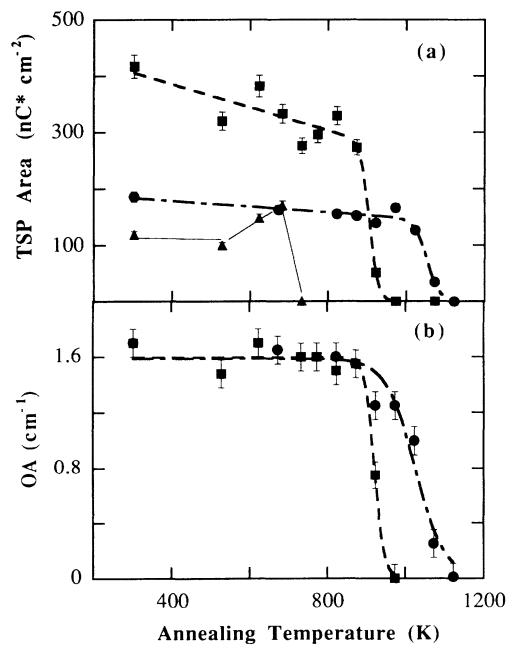


FIG. 8. (a) Annealing curves for the TSP process *B* induced by quenching in air from 1270 K (\blacktriangle), 1570 K (\blacksquare), and 1920 K (\bullet) ($V_p = 25$ V). (b) Annealing curves for the 480-nm optical-absorption band induced by quenching in air from 1570 K (\blacksquare) and 1920 K (\bullet).

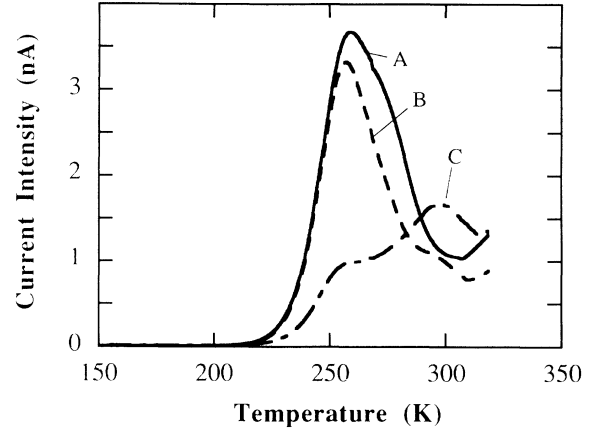


FIG. 9. TSP spectra in a sample quenched in air from 1920 K and thermally annealed up to 1070 K, obtained with electrodes covering almost all sample area (*A*), only the sample colored region (*B*), and only the colorless region (*C*).

The pulsed thermal annealing measurements are shown in Fig. 8 for three samples, each one quenched from a different temperature up to saturation conditions. The thermal annealing of the TSP *B* process occurs in a single step which coincides in each case with that of the 480-nm optical-absorption band (the annealing curve for this band in the sample quenched from 1270 K is not plotted because of its very low amplitude, which causes errors to be very large). An important feature is that the higher the quenching temperature the higher the annealing temperature. Peak *A* and the HT region decay together with peak *B*.

At the last part of the annealing step some samples became colorless starting from their edges, as was also observed by Wang *et al.*¹ For a detailed study of the behavior in this last stage, the TSP spectrum was measured with small electrodes only covering either the colored or the colorless sample area. As shown in Fig. 9, in the colorless area a broad TSP band peaking at about 300 K is dominant, having a shoulder at around 270 K, which is the position of the TSP peak in the colored region. The TSP spectrum measured with an electrode covering the complete sample face obviously shows the contributions of both the colored and the colorless regions.

E. Current-voltage characteristics at room temperature

In order to investigate electrode effects, the current-voltage characteristics of the electrical conduction were measured. As it was also observed in MgO:Li ,¹³ there is a highly nonlinear electrical conductivity at room temperature. Some effects make the measurements difficult: when the voltage is applied the current does not remain constant, but slowly grows up to a given value. On a subsequent reduction of the voltage, the current intensity always remains larger than that observed in the previous increasing voltage sweep. A further increasing sweep leads to almost the same values as those obtained during the decreasing one. Therefore, the experimental values in the current-voltage curve shown in Fig. 10 correspond to

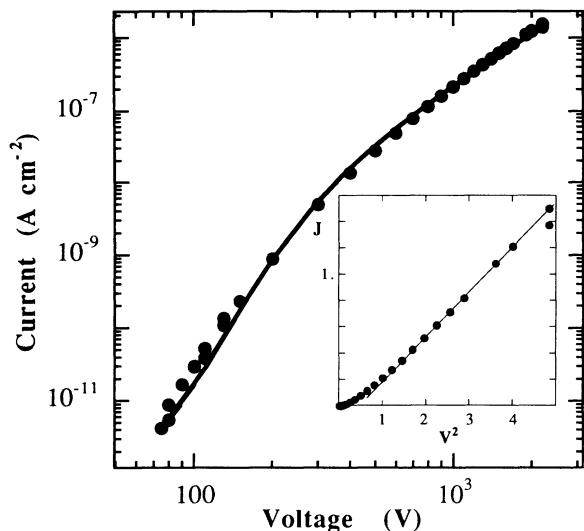


FIG. 10. Current-voltage curve at room temperature of $\text{Al}_2\text{O}_3:\text{Mg}$ with plain electrodes. The full line is the fitting to Eqs. (1) and (2) (see text). The inset shows this curve plotted as I against V^2 .

this last situation. The curves are symmetric for both positive and negative bias when plain electrodes are used on both sample faces. Attempts to fit these curves to the equations governing electrode-limited- or bulk-limited-conduction mechanisms gave good results only in two cases. On one hand, the plot of $\ln(I/V^2)$ against $1/V$ (I being the measured electric-current intensity and V the applied voltage) can be well fitted to a straight line, suggesting that the current-voltage curves might follow the Fowler-Nordheim equation, that is, field emission from the electrode might take place.¹⁴ Nevertheless, this can be rejected because calculations show that either the barrier height would be too low or the acceptor-center concentration would be too high. On the other hand, it has also been found that I is proportional to V^2 in the high-voltage range (see the inset in Fig. 10). However,

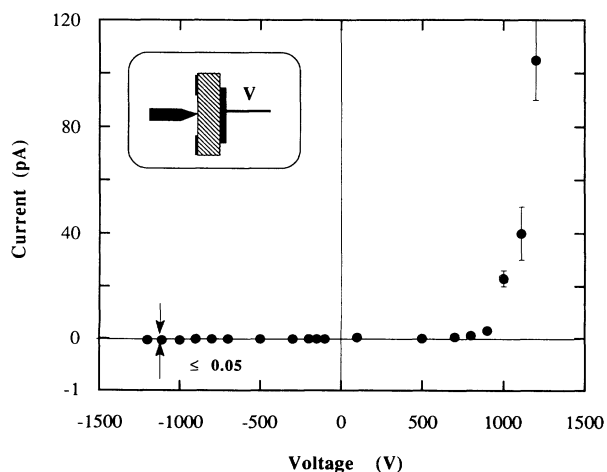


FIG. 11. Current-voltage curve of a sample with a tip electrode on one face and a plain one on the other.

the overall curve fits well to the combination of two terms, one of them being proportional to $\exp(V^{1/4})$ and the other to V^2 . The significance of this fitting shall be discussed in the next section.

The I - V curve was also obtained with a tip electrode on one sample face and a plain electrode on the other. The obtained curve is clearly not symmetric (see Fig. 11) showing a behavior similar to that of a Schottky diode.¹⁵ The system is conducting when the tip electrode is negatively biased.

IV. DISCUSSION

The role played by magnesium ions has been clearly put in evidence from the close parallelism between the behavior of the main TSP-TSD process and that of the 480-nm optical-absorption band, which is due to $\text{Mg}_{\text{Al}}^{\text{x}}$ centers. These are well-known hole centers responsible for the 220-K thermoluminescence peak that appears in $\text{Al}_2\text{O}_3:\text{Mg}$ x-irradiated at 77 K.³ It is also clear that dipolar reorientation processes cannot account for the huge TSP current intensity: from the total magnesium concentration in our samples, the peak B intensity should be about 10^3 – 10^4 times lower than the measured one if all magnesium ions were involved in those dipoles. Then charge migration must occur over rather long distances as compared to the unit cell. A good agreement is found between the activation energy obtained in this work (from both the TSP and the isothermal measurements) and the energy for thermally activated hole release from $\text{Mg}_{\text{Al}}^{\text{x}}$ centers found in ESR, thermoluminescence, and thermally stimulated exoelectron-emission studies.^{1,3,4} So it can be concluded that we are dealing with a polarization process caused by a limited hole conduction process, the $\text{Mg}_{\text{Al}}^{\text{x}}$ centers being the carriers' source. This conclusion is also supported by the results obtained in studying the I - V characteristics using one tip electrode (Fig. 11): The current direction is consistent with the electric carriers being holes.

As was mentioned in the Introduction, Eisenberg *et al.*⁸ proposed that the polarization and depolarization processes observed in quenching $\text{MgO}:\text{Li}$ take place inside inclusions (or microgalaxies) containing a high density of substitutional lithium ions. According to these authors, since hole exchange between $\text{Li}_{\text{Mg}}^{\text{x}}$ and Li'_{Mg} centers occurs because the former can be thermally ionized below room temperature, these inclusions are polarizable semi-conducting regions inside an insulating matrix. This leads to Maxwell-Wagner polarization phenomena.¹⁶ Nevertheless, although there is clear evidence that the $\text{Mg}_{\text{Al}}^{\text{x}}$ centers in $\text{Al}_2\text{O}_3:\text{Mg}$ behave as the $\text{Li}_{\text{Mg}}^{\text{x}}$ centers in $\text{MgO}:\text{Li}$ and therefore, microgalaxies of $\text{Mg}_{\text{Al}}^{\text{x}}$ centers in $\text{Al}_2\text{O}_3:\text{Mg}$ can be assumed to be formed, some of our experimental results indicate that a Maxwell-Wagner process can be disregarded as being the origin of the main polarization process (that leading to TSP peak B) in $\text{Al}_2\text{O}_3:\text{Mg}$. First, the results plotted in Fig. 6 show that the peak B area, i.e., the total polarization P_0 (total charge per unit electrode area), increases almost linearly with $V_p^{1/2}$, while one would expect a linear dependence on V_p in TSP and TSD processes due either to dipolar reori-

entation or Maxwell-Wagner polarization.^{7,17} On the other hand, P_0/E_p (that is, the increase in the sample dielectric constant due to the polarization process related to peak *B*) is dependent on the sample thickness, as seen in Fig. 5. In other words, the sample capacitance P_0/V_p is thickness independent. This result is particularly important since it shows that peak *B* cannot arise from either a Maxwell-Wagner or a dipolar process but it is associated with the electrode contact region.¹⁸⁻²⁰ So it is sensible to conclude that electric-charge accumulation at one electrode occurs, i.e., the electrodes make blocking contacts for holes with the insulator.

The results obtained from the study of the current-voltage characteristics also support this conclusion. It has been shown on one hand that the system behaves as a Schottky diode when a tip electrode is used on one sample face. On the other, when both electrodes are plain, the electric-current intensity as a function of the applied voltage can be described by the following system of equations:

$$J = J_{c0} \exp(\alpha_c V_c^{1/4}), \quad (1)$$

$$J = J_{b0}(V - V_c)^2, \quad (2)$$

where V_c and $(V - V_c)$ are the voltage drops across the contact and the bulk, respectively. J_{b0} , J_{c0} , and α_c are constants for each sample and temperature. The first expression is the Richardson-Schottky equation and represents the dominant behavior at low voltages. This is consistent with the formation of a Schottky barrier at the sample surface.^{19,21} The second expression, which dominates at high voltages, is the Mott-Gurney equation for a space-charge-limited conduction process.²² The whole behavior agrees with the occurrence of an electrode-limited to bulk-limited transition in the conduction process. It has been shown that such a transition can take place at some sufficiently high voltage when Schottky barriers exist at the contact.^{14,20} The transition occurs when the contact resistance decreases to values comparable to the bulk resistance as the voltage increases, so the limiting factor is no longer the Schottky barrier but the electrostatic repulsion of the injected charge.

The experimental values for the band gap of Al_2O_3 vary between 8.7 and 9.5 eV,^{23,24} its electron affinity being 1 eV.²⁵ Then the work function of $\text{Al}_2\text{O}_3:\text{Mg}$ -containing Mg_{Al}^x centers lies between 6 and 10 eV, depending on the exact position of the Fermi level. These values are greater than the work function of any of the metals used for the electrodes, which is 4.12 eV for indium, 5.65 eV for platinum, 5.10 eV for gold, and 4.28 eV for aluminum.²⁶ This lends further support to the existence of blocking contacts for holes. Figure 12 presents the expected energy-band diagram for our metal-insulator-metal system.

Thermally stimulated polarization and depolarization processes in metal-insulator-metal systems with blocking contacts can be studied using the stimulated dielectric-relaxation-currents (SDRC) theory developed by Simmons and Taylor.^{27,28} The existence of blocking contacts for holes causes a depletion region with a negative space charge (ionized acceptors) to be formed at the electrode-

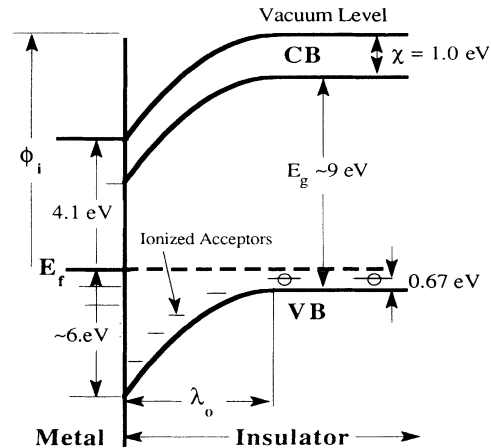


FIG. 12. Energy-band diagram at the metal-insulator interface for indium electrodes. λ_0 is the width of the depletion region.

insulator interfaces due to hole escape from traps near the sample surfaces. When a voltage is applied at a sufficiently high temperature, the metal-insulator-metal system relaxes to the so-called steady state²⁷ because of the growth of the anodic depletion region caused by a further hole escape. Thus a time-dependent-relaxation current is observed, the steady state being reached when the current is spatially or temporally constant throughout the system. In TSP measurements the voltage is applied at low temperature, at which the emission coefficient for hole release from traps is negligible, therefore, no current can be observed. As the temperature is raised at a constant rate this coefficient increases, the holes start to be released when it approaches a value of about 10^{-2} . The relaxation current versus temperature curve is peak shaped, and the current ceases to flow when all the traps in the region corresponding to the steady-state anodic depletion region have been depleted of their holes. The system is now in the steady state and, hence, the current flowing in the system is the steady-state current.²⁸ In the TSD case the sample temperature is first lowered with the voltage on; thus, the system remains in its steady state at low temperature. In the subsequent heating run with the electrodes short-circuited the system begins to relax when the temperature becomes sufficiently high. It first relaxes to an intermediate state called the quasisteady state,²⁷ this relaxation gives rise to a current versus temperature peak similar to the TSP case. At higher temperatures it relaxes again from this state to the steady state, a second peak being observed if the two electrode-insulator interfaces are not identical.²⁸

Besides the already-mentioned fact of the thickness dependence of the TSP area, other experimental results in this work agree with predictions of this SDRC theory.

(i) High-voltage TSP measurements (Fig. 3) show, after peak *B*, the steady-state current growing with the temperature.²⁸ This is not clearly seen in low-voltage measurements because of the highly nonlinear characteristics of the current-voltage curves. In the second heating run

only the steady-state current appears (see Fig. 3), as expected from the fact that the applied voltage during cooling is the same as during heating.^{20,28} Also, the fitting method used to calculate the activation parameters as well as the isothermal-polarization-current measurements have revealed that peak *B* is related to a first-order-kinetics process, as the theory predicts assuming that re-trapping in the depletion region is negligible.²⁸

(ii) One of the findings of this theory is the fact that the relaxation time, and thus, T_m in TSP measurements, increases with the sample thickness.²⁷ This has been observed here experimentally.

(iii) It was found that the electric charge Q released during a TSP process is approximately proportional to $V_p^{1/2}$. As it can be seen in Fig. 6, the Q versus V_p curve can actually be well fitted to the following equation:

$$Q = (2\epsilon N_t)^{1/2} [(\Delta\Psi + qV_p)^{1/2} - \Delta\Psi^{1/2}], \quad (3)$$

where $\Delta\Psi$ is the difference in work function between the metal and the insulator, ϵ is the permittivity, and N_t the concentration of acceptor centers. This is the equation predicted by the SDRC theory.²⁸ From this equation the acceptor center density near the depletion region can be calculated. Values ranging between $5 \times 10^{15} \text{ cm}^{-3}$ (0.1 ppm approximately) for as-cut samples and $5 \times 10^{16} \text{ cm}^{-3}$ (1 ppm approximately) for quenched samples are obtained. These are in good agreement with both the total magnesium concentration of our samples and the $\text{Mg}_{\text{Al}}^{\text{x}}$ -center concentration measured by optical absorption, which give upper limits.

(iv) On the other hand, the charge involved in the TSP measurements is much greater (by about 1000 times) than that corresponding to the geometrical capacitance of the sample, as the theory states.²⁷ This is due to the fact that almost all the applied voltage drops across the depletion layer, hence, the depletion width, instead of the sample thickness, is involved. From the obtained capacitances, this depletion width has been estimated to be in the range 0.6–7 μm , for different sample treatments.

(v) As was mentioned before, hysteresis and “memory effects” appear when measuring consecutive TSP-TSD spectra: for example, a second TSP run made just after a first one always gives lower polarization values; also TSD peaks are smaller than TSP peaks for the same experimental conditions. These effects, which cannot be explained in the frame of dipolar reorientation or Maxwell-Wagner polarization phenomena, are natural consequences of this theoretical framework. They can be well understood by considering that the cathode, contrary to the anode, is forward biased under polarization and then offers a low-resistance path to hole current. When the sample is polarized at high temperature the net effect is a charge leakage. On switching off the applied voltage both depletion regions behave as blocking contacts, since hole injection from the electrodes to the sample must overcome the Schottky barrier. Therefore, although the charge distribution inside the sample relaxes to a symmetric state, the Fermi level is not at the equilibrium value. This is the so-called quasisteady state. Hysteresis occurs when the heating process is interrupted at a tem-

perature just above that at which the system relaxes to the quasisteady state (this is our experimental case since the upper limit in temperature of our cryostat is near the end of peak *B*). In this condition, if the electrode barriers are quite high, the system would require a very long period of time to relax to the steady state after switching off the applied voltage in the case of a TSP measurement (similarly it can be seen that the final state in the case of a TSD measurement would be the quasisteady state and not the steady state). Then the charge involved in the second TSP run is lower than that involved in the first run by an amount of $Q_s/2$, Q_s being the charge that escaped from the sample during the previous polarization and was not recovered. The experimental consequence is that charge values depend upon the total history of the sample (polarization voltages, maximum temperatures reached, elapsed time between measurements). So care must be taken when calculating microscopical parameters or displaying Q - V curves. This is the reason why sample-to-sample comparisons have been made from the first TSP run in freshly quenched samples and Q - V curves were obtained for increasing voltage polarization in order that the final state was always the steady state.

The same mechanism may be invoked in order to explain the hysteresis effect observed in the current-voltage curves at room temperature. Charge leakage from the sample induces a higher field at the anodic region and, therefore, a higher emission current than that corresponding to the equilibrium state. Another mechanism could be the near-interface-trapped-charge modification giving rise to a slow current increase at constant bias, as observed in many metal-semiconductor contacts.²⁹

From all the above considerations it can be concluded that the main TSP-TSD peak observed in $\text{Al}_2\text{O}_3:\text{Mg}$ is due to the stimulated dielectric-relaxation currents appearing in a metal-insulator-metal system with blocking contacts at the metal-insulator interfaces. In our case the centers involved in the relaxation process are the $\text{Mg}_{\text{Al}}^{\text{x}}$ centers inside the microgalaxies, which are formed by oxidizing quenching from magnesium-aluminum-spinel precipitates, as proposed by Wang *et al.*¹ These precipitates have been observed to be present in our samples by scanning electron microscopy.

Nothing conclusive can be said from our results for the dependence of T_m on V_p . Poole-Frenkel lowering of the donor barrier (in the case of charge carriers being electrons) was proposed to explain a similar behavior in other systems.¹⁹ Another possible explanation might come from the strong voltage dependence of the carrier mobility in hopping systems.³⁰ The variations of T_m with the quenching temperature and with the heating time before quenching cannot yet be explained.

Peak *A* and the HT region are closely related to peak *B* since they are induced together by the same sample treatments and they anneal out at the same time. Moreover, the height ratio of peak *B* to the HT region is similar among all measurements. Only few data have been obtained because of the experimental difficulties already mentioned. The area of peak *A* seems to grow linearly with the applied voltage and the temperature at the maximum is rather constant when the experimental condi-

tions are varied. This peak could then be due to Maxwell-Wagner polarization of microgalaxies, as it was proposed for the main TSD peak in MgO:Li.⁸ As the conductivity is expected to be higher inside the inclusions, and shorter distances are involved, this process should occur at a lower temperature than the interface polarization, as it has been observed in this work.

The HT region is a composed peak, as thermal sampling measurements show. Although results of Fig. 9 might indicate that it is not directly related to Mg_{Al}^x centers, these can still be present (but not being observable by optical absorption) in the colorless area of the partially annealed sample, where the HT region dominates in the TSP and TSD spectra. In fact, Wang *et al.*¹ detected these centers by ESR, but not by optical absorption, in the colorless area of a sample treated as ours. The HT region cannot be ascribed to the relaxation of the quasisteady state to the steady state because it should have only been observed in TSD measurements.²⁸ A unique model for this process cannot be proposed at the present time. A possibility is that it might be ascribed to a Cottrell-like atmosphere induced by impurities around dislocations, as it has been proposed to explain a TSD

peak in LiF:Ti.³¹ A second possibility is that holes leaving the microgalaxy are trapped in deeper centers with an energy distribution.

The results of Fig. 8 show that the thermal stability of the quenching-induced Mg_{Al}^x centers and of the TSP processes is higher when the quenching temperature is increased. This might indicate that the larger microgalaxies are more thermally stable than the smaller ones, in good agreement with theoretical calculations by Foot, Colburn, and Catlow³² for MgO:Li. Indeed Wang *et al.*¹ observed that Mg_{Al}^x centers produced by quenching from temperatures well above 1850 K cannot be thermally annealed.

Finally, it should be pointed out that the concepts presented here would also be applicable to other wide-band-gap-insulating materials containing hole centers.

ACKNOWLEDGMENT

We are indebted to Dr. B. Salce (C.E.N. Grenoble, France) for supplying the samples used in this work.

¹H. A. Wang, C. H. Lee, F. A. Kröger, and R. T. Cox, *Phys. Rev. B* **27**, 3821 (1983).
²R. T. Cox, *Solid State Commun.* **9**, 1989 (1971).
³P. A. Kulis, M. J. Springis, I. A. Tale, V. S. Vainer, and J. A. Valbis, *Phys. Status Solid B* **104**, 719 (1981).
⁴V. S. Kortov, T. S. Bessonova, M. S. Akselrod, and I. I. Milman, *Phys. Status Solid A* **87**, 629 (1985).
⁵F. A. Kröger and H. J. Vink, in *Solid State Physics*, edited by F. Seitz and D. Turnbull (Academic, New York, 1956), Vol. 3, p. 307.
⁶Y. Chen, H. T. Tohver, J. Narayan, and M. M. Abraham, *Phys. Rev. B* **16**, 5535 (1977).
⁷C. Bucci, R. Fieschi, and G. Guidi, *Phys. Rev.* **148**, 816 (1966).
⁸D. J. Eisenberg, L. S. Cain, K. H. Lee, and J. H. Crawford, Jr., *Appl. Phys. Lett.* **33**, 479 (1978).
⁹R. Vila, A. Ibarra, and M. Jiménez de Castro, *Phys. Status Solidi A* **105**, 601 (1988).
¹⁰A. K. Jonscher, *Dielectric Relaxation in Solids* (Chelsea, London, 1983).
¹¹H. Kleim, R. Schmidt, and G. Artl, *J. Appl. Phys.* **53**, 1590 (1982).
¹²R. Vila and M. Jiménez de Castro, *Radiat. Eff. Def. Solids* **119-121**, 609 (1991).
¹³Y. Chen, R. H. Kernohan, J. L. Boldu, M. M. Abraham, D. J. Eisenberg, and J. H. Crawford, Jr., *Solid State Commun.* **33**, 441 (1980).
¹⁴J. G. Simmons, *Phys. Rev.* **166**, 912 (1968).
¹⁵E. H. Rhoderick and R. H. Williams, *Metal-Semiconductor*

Contacts (Clarendon, Oxford, 1988).
¹⁶L. K. H. Van Beek, *Physica* **26**, 66 (1960).
¹⁷R. Vila and M. Jiménez de Castro, *J. Phys. D* **25**, 1357 (1992).
¹⁸P. Müller, *Phys. Status Solidi A* **67**, 11 (1981).
¹⁹G.S. Nadkarni and J. G. Simmons, *J. Appl. Phys.* **43**, 3650 (1972).
²⁰J. G. Simmons and G. S. Nadkarni, *Phys. Rev. B* **6**, 4815 (1972).
²¹J. G. Simmons and G. S. Nadkarni, *Phys. Rev. B* **12**, 5459 (1975).
²²N. F. Mott and R. W. Gurney, *Electronic Processes in Ionic Crystals* (Dover, New York, 1964).
²³M. L. Boltz and R. H. French, *Appl. Phys. Lett.* **55**, 1955 (1989).
²⁴W. H. Strehlow and E. L. Cook, *J. Phys. Chem. Ref. Data* **2**, 163 (1973).
²⁵C. R. Viswanathan and R. Y. Loo, *Appl. Phys. Lett.* **21**, 370 (1972).
²⁶H. B. Michaelson, *J. Appl. Phys.* **48**, 4729 (1977).
²⁷J. G. Simmons and G. W. Taylor, *Phys. Rev. B* **6**, 4793 (1972).
²⁸J. G. Simmons and G. W. Taylor, *Phys. Rev. B* **6**, 4804 (1972).
²⁹A. Thanailakis and D. C. Northrop, *J. Phys. D* **4**, 1776 (1971).
³⁰I. Chen, *J. Appl. Phys.* **47**, 2988 (1976).
³¹R. Capelletti, C. Mora, G. Ruani, I. Földvári, L. Kovács, and A. Watterich, *Cryst. Lattice Defects Amorph. Mater.* **16**, 153 (1987).
³²J. D. Foot, E. A. Colbourn, and C. R. A. Catlow, *J. Phys. Chem. Solids* **49**, 1225 (1988).